Supporting Information

Introducing Oxygen Vacancies to NiFe LDH through Electrochemistry Reduction to Promote Oxygen Evolution Reaction

Xiaoman Hou [a], Jing Li [b], Jian Zheng [a], Luming Li [c] and Wei Chu *[a]

Experimental and Characteristics

Comparison experiment

1. Different methods to prepare NiFe LDH:

(1) Hydrothermal method (HT): Disperse $Ni(NO_3)_2·6H_2O$ (1.890 g), $Fe(NO_3)_3·9H_2O$ (0.263 g) and precipitation agent urea (8.64 g) in deionized water (120 mL), and stirred for 15 min to obtain transparent solution, then transferred to a Teflon-lined stainless steel autoclave treated at 120 °C for 12 h. The power was collected by repetitive centrifugation at 8000 rpm for 3 min and washed several times by H_2O and EtOH, then dried at 60 ℃ in oven for 24 h.

(2) Co-precipitation (CP): Disperse $Ni(NO_3)_2·6H_2O$ (1.890 g), $Fe(NO_3)_3·9H_2O$ (0.263 g) in deionized water (120 mL) and stir to form a transparent metal salt solution. In a 60 ℃ water bath, slowly drip the metal salt solution and 1 M NaOH solution into 50 mL 0.15 M Na_2CO_3 solution under stirring, and control the pH value of the solution to about 10±0.5. After the dropwise addition of the metal salt solution was completed, the precipitate was aged at 60°C for 18 hours. The power was collected by repetitive centrifugation at 8000 rpm for 3 min and washed several times by H_2O and EtOH, then dried at 60 ℃ in oven for 24 h.

2. Preparation of MN LDH (M, N = Ni, Co, Fe)

NiCo LDH, CoFe LDH, and NiCoFe LDH were synthesized by microwave heating method as the synthesis of NiFe LDH. Among them, except for the change in the quality of the metal salt, the other experimental conditions remain the same. $Ni(NO_3)_2·6H_2O$ is 0.419 g and $Co(NO_3)_2·6H_2O$ is

[a] College of Chemical Engineering, Sichuan University, Chengdu 610065, China. E-mail: chuwei1965@scu.edu.cn.
[b] Department of chemistry, Tsinghua University, Beijing 100084, China.
[c] Institute for Advanced Study, Chengdu University, Chengdu 610106, China.

1.676 g in NiCo LDH. $Co(NO_3)_2 \cdot 6H_2O$ is 1.892 g and $Fe(NO_3)_3 \cdot 9H_2O$ is 0.263 g in CoFe LDH. $Ni(NO_3)_2 \cdot 6H_2O$ is 0.378 g, $Co(NO_3)_2 \cdot 6H_2O$ is 1.513 g, $Fe(NO_3)_3 \cdot 9H_2O$ is 0.263 g in NiCoFe LDH. The molar ratio of metal salt is the optimal ratio determined by our previous work.

3. Preparation of NiFe LDH/X (X = Cu Foam, carbon cloth)

NiFe LDH/Cu Foam (CF, 1×1 cm^2) and NiFe LDH/Carbon Cloth (CC, 1×1 cm^2) were prepared by replacing NF substrate. The method was the same as the synthesis of NiFe LDH/NF.

Calculation of Faradaic Efficiency

The Faradaic Efficiency of OER was estimated using the following equation:

$$FE = 4Fn_{O2}/It \times 100\%$$

Where F is Faraday constant (96485 C/mol), n_{O2} is the number of moles of experimental O_2 during the reaction (mol), I is the current of the reaction (A), t is the reaction time (s).

Tafel slope measured by steady-state polarization

In order to compare with the Tafel slope calculated by the LSV curve, the steady-state method is used to measure Tafel slope. Set the voltage and reaction time by potentiostatic method to measure the current density at a steady state. Then the logarithm of the current density ($\log|j|$) at steady state is plotted against the overpotential (η), and the Tafel slope can be obtained by fitting linear curves, as shown in Fig. S17.

ICP-MS measurement

The content of Ni and Fe in the KOH solution of r-NiFe LDH before and after 1000 CV cycles were measured by ICP-MS, as shown in Table S3. The content of Ni and Fe have a very small increase that can be ignored, indicating r-NiFe LDH has excellent stability.

Figures and Tables

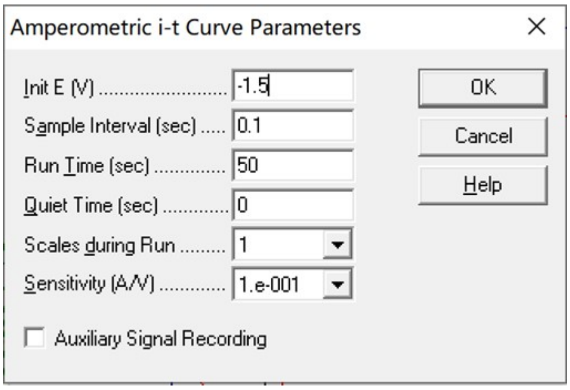

Fig. S1 Schematic diagram of parameter setting of I-T (-1.5 V，50 s)

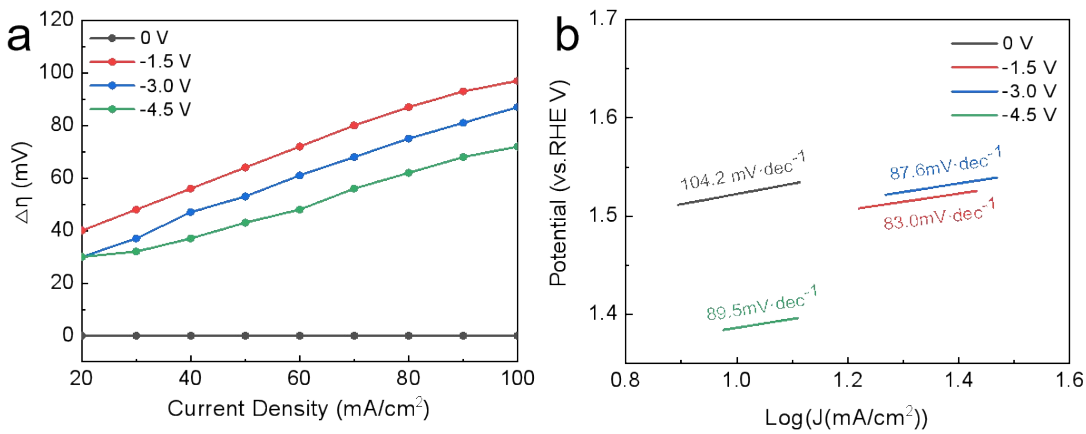

Fig. S2 Samples of different reduction potential (a) Δη-j chart, (b) Tafel plots

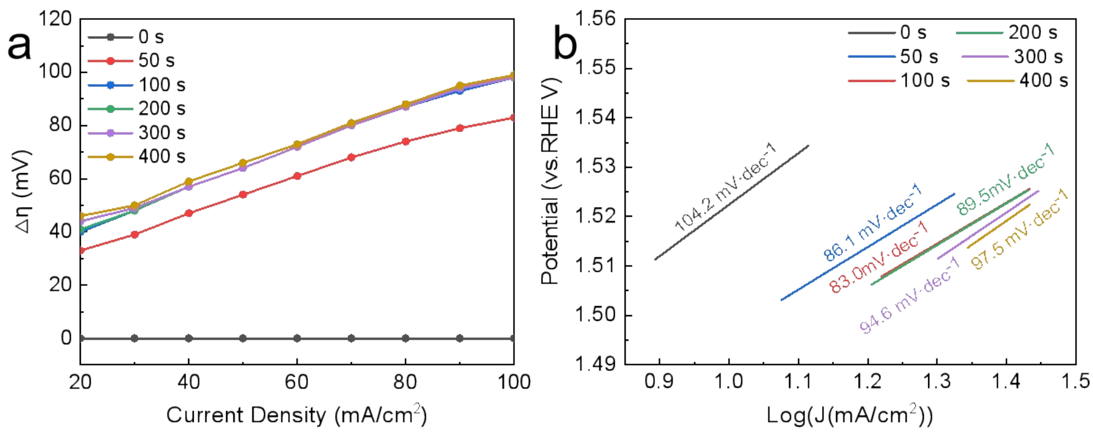

Fig. S3 Samples of different reduction time (a) Δη-j chart, (b) Tafel plots

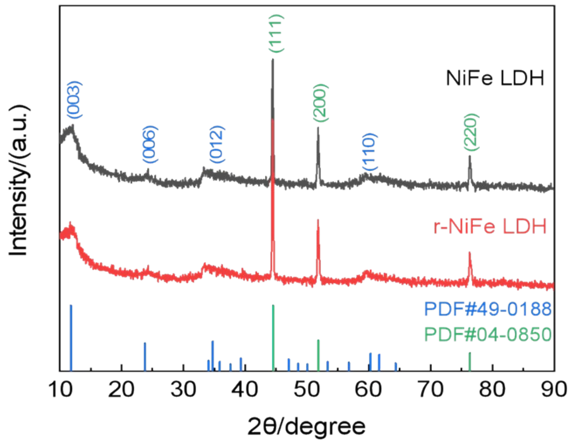

Fig. S4 XRD patterns of NiFe LDH and r-NiFe LDH

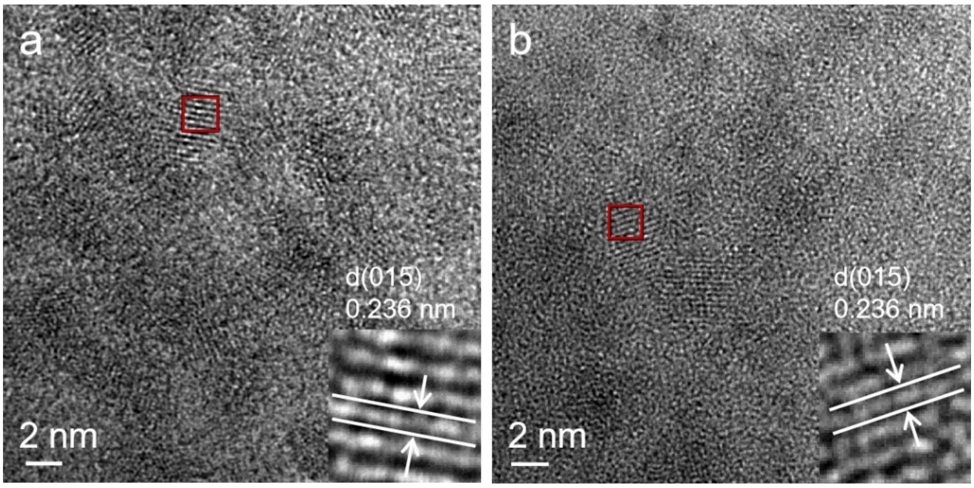

Fig. S5 HRTEM image of (a) NiFe LDH and (b) r-NiFe LDH

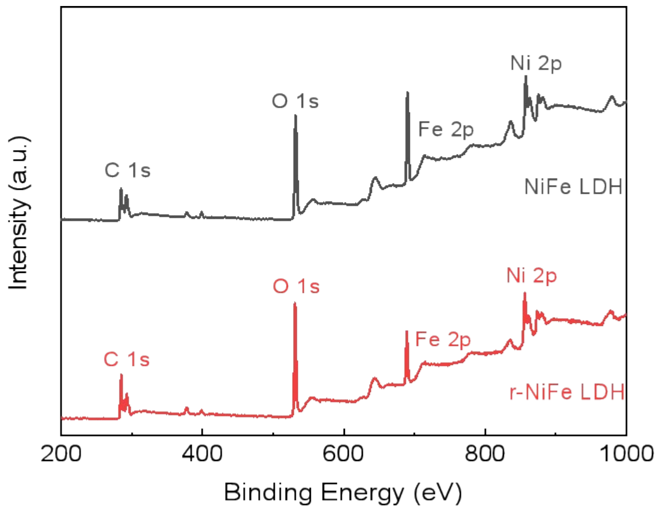

Fig. S6 XPS spectra of NiFe LDH and r-NiFe LDH

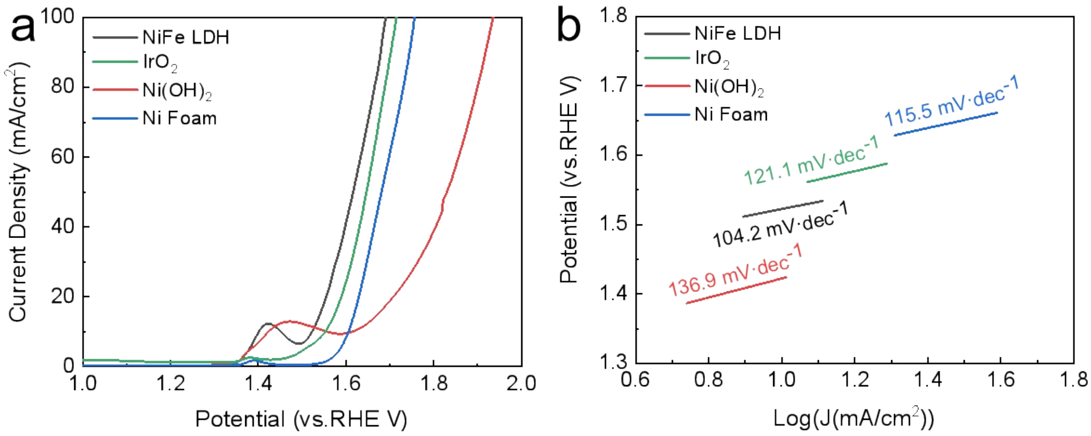

Fig. S7 Comparison samples (a) LSV curves, (b) Tafel plots

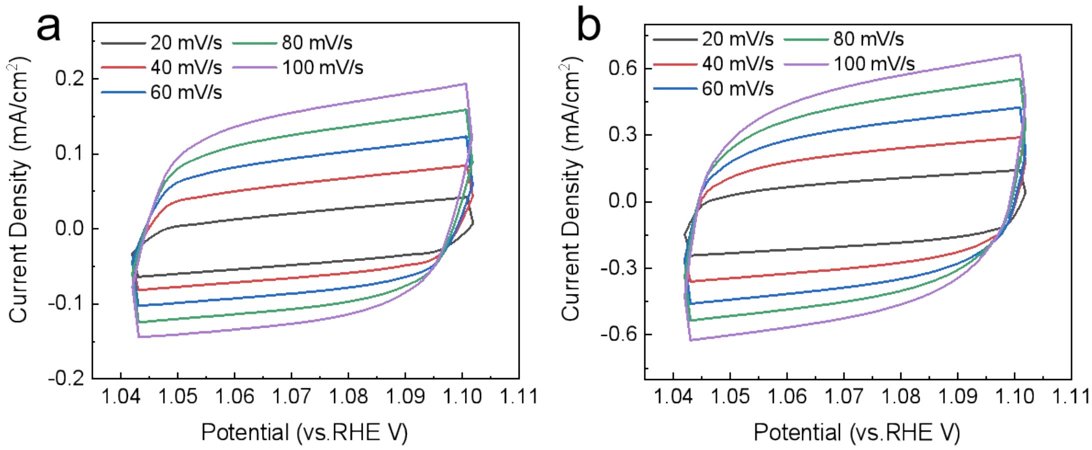

Fig. S8 The CV curves at different scan rates (20, 40, 60, 80, 100 mV/s) of (a) NiFe LDH and (b) r-NiFe LDH

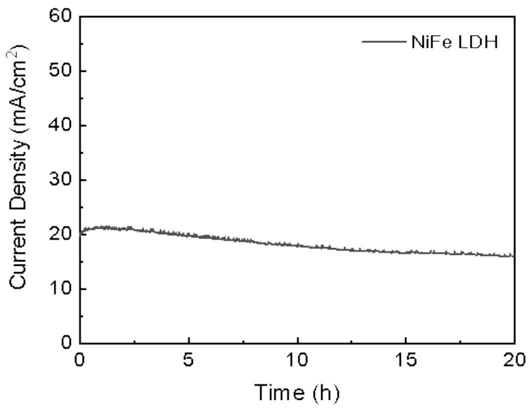

Fig. S9 Stability test of NiFe LDH at current density of 20 mA·cm^{-2}

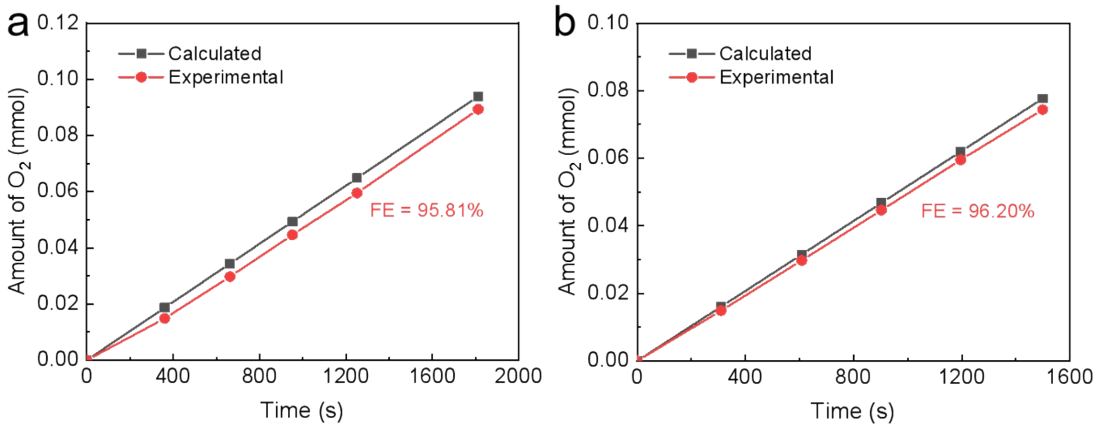

Fig. S10 The amount of O_2 theoretically calculated and experimentally measured versus time at current density of 20 mA·cm^{-2} : (a) NiFe LDH, (b) r-NiFe LDH

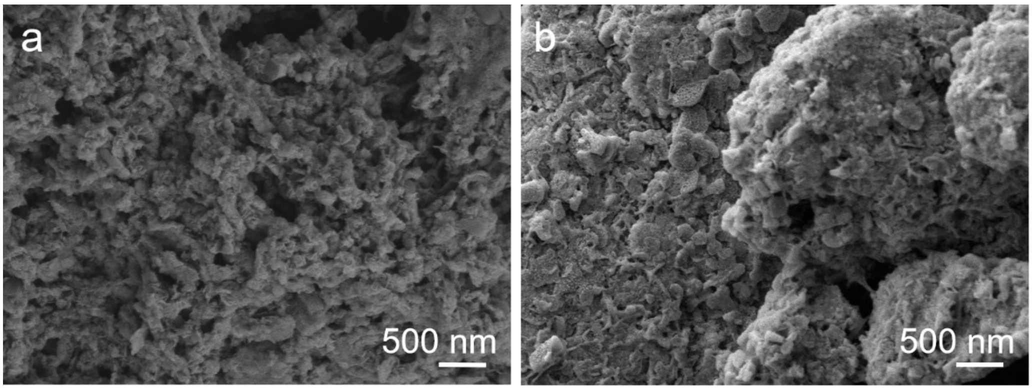

Fig. S11 SEM images of r-NiFe LDH (a) before and (b) after stability test

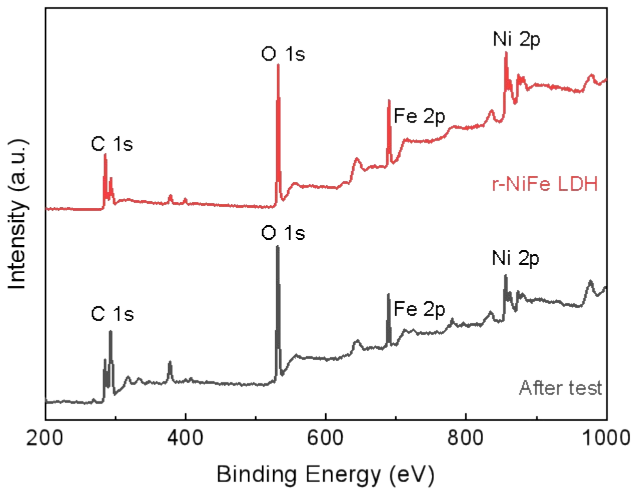

Fig. S12 XPS spectra of r-NiFe LDH before and after stability test

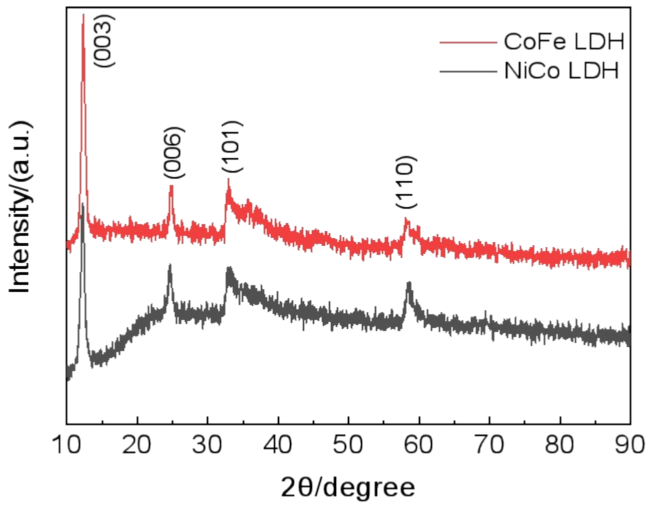

Fig. S13 XRD patterns of CoFe LDH and NiCo LDH

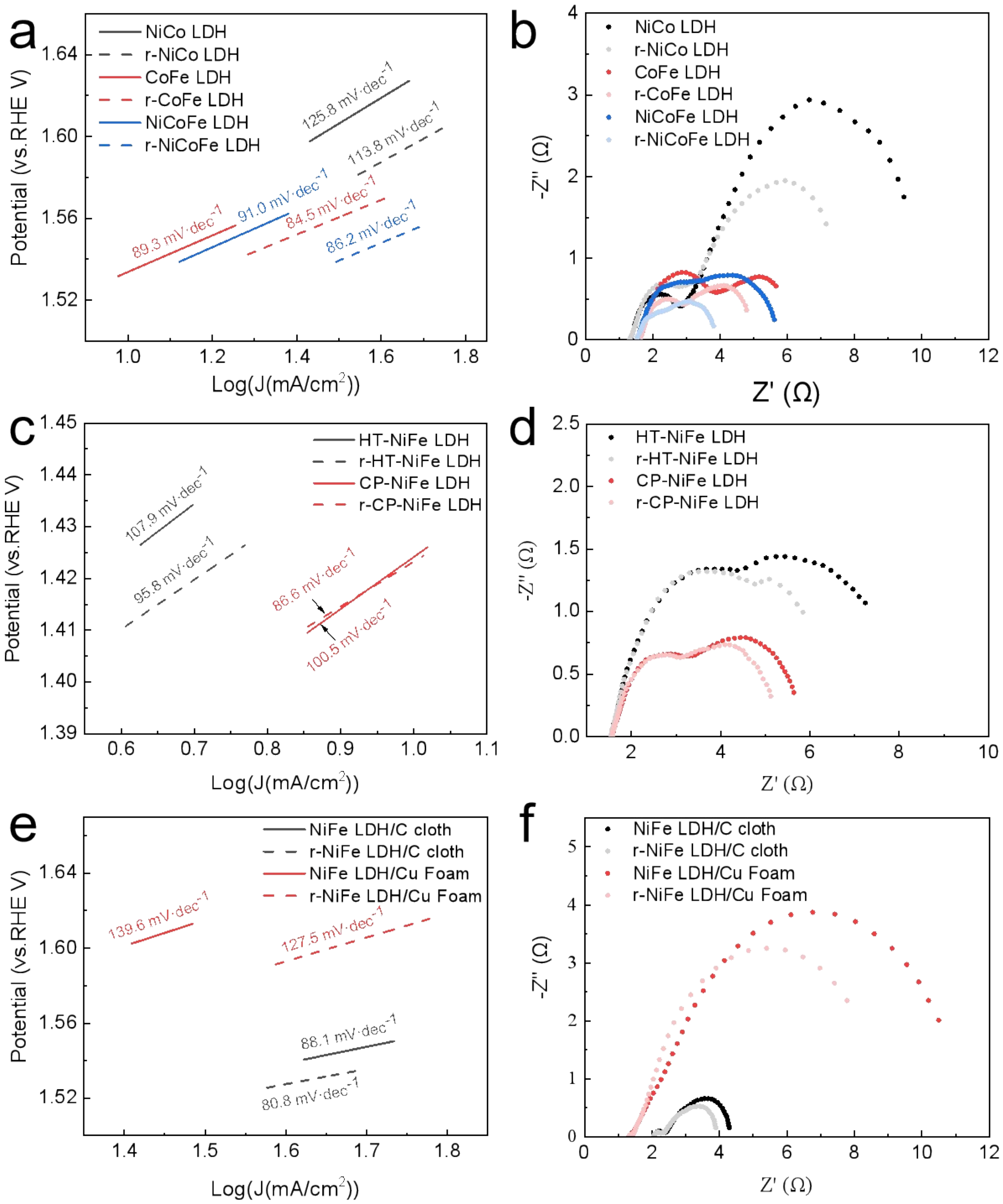

Fig. S14 The Tafel plots of (a) MN LDH (M, N = Ni, Co, Fe), (c) NiFe LDH synthesized by hydrothermal method and co-precipitation method, (e) NiFe LDH/X (X = Carbon Cloth, Cu Foam); The EIS curves of (b) MN LDH (M, N = Ni, Co, Fe), (d) NiFe LDH synthesized by hydrothermal method and co-precipitation method, (f) NiFe LDH/X (X = Carbon Cloth, Cu Foam).

Table S1 Comparison of OER performance for the present catalyst with some catalysts reported in the literature.

Catalyst	Overpotential@ Density Current (mV@ $mA\cdot cm^{-2}$)	Tafel slope ($mV\cdot dec^{-1}$)	Substrate	Refs.
r-NiFe LDH	285@20	83.0	Ni Foam	This work
r-NiFe LDH	305@50	80.8	Carbon Cloth	This work
Fe-$Ni(OH)_2$	285@50	223.5	Ni Foam	[1]
$Ni_{1-x}Fe_xOOH$	320@10	/	Au discs	[2]
NiFe LDH-PANI	220@10	44	Carbon Paper	[3]
NiFe LDH	260@10	55	Carbon Paper	[3]
NiFe-MOF	215@10	49.1	/	[4]
$NaBH_4$-NiFe LDH	280@10	56	Ni Foam	[5]
$NiFe_2O_4$	324@10	132	Ni Foam	[6]
NiFe-LDH/CF	382@10	124	Carbon Fiber	[7]
A-NiFeLDH	241@10	55	Glassy Carbon	[8]
nNiFe LDH/3D MPC	340@10	71	/	[9]
NiFeMn-LDH	289@20	47	/	[10]
Fe-CoOOH/G	330@10	37	GO	[11]
NiCoFe-LDH	276@10	56	Ni Foam	[12]
NiFeLDH/NiTe	228@50	51.04	Ni Foam	[13]
$Ni_3N@Fe_3N$	296@10	40	Carbon Fiber	[14]
$Ni_{1.5}Fe_{0.5}P$/CF	264@10	55	Carbon Fiber	[15]
V10-Ni_2P	308@10	75.1	Glassy Carbon	[16]
NiFe-Se/CFP	281@10	40.93	Carbon Fiber Paper	[17]

Table S2 Equivalent analog circuit parameters of NiFe and r-NiFe

Samples	Rs ($\Omega\cdot cm^{-2}$)	CPE1 ($F\cdot cm^{-2}$)	R1 ($\Omega\cdot cm^{-2}$)	CPE2 ($F\cdot cm^{-2}$)	R2 ($\Omega\cdot cm^{-2}$)
NiFe LDH	1.305	0.0067856	1.296	0.063453	2.581
r-NiFe LDH	1.415	0.16889	0.76093	0.10149	1.313

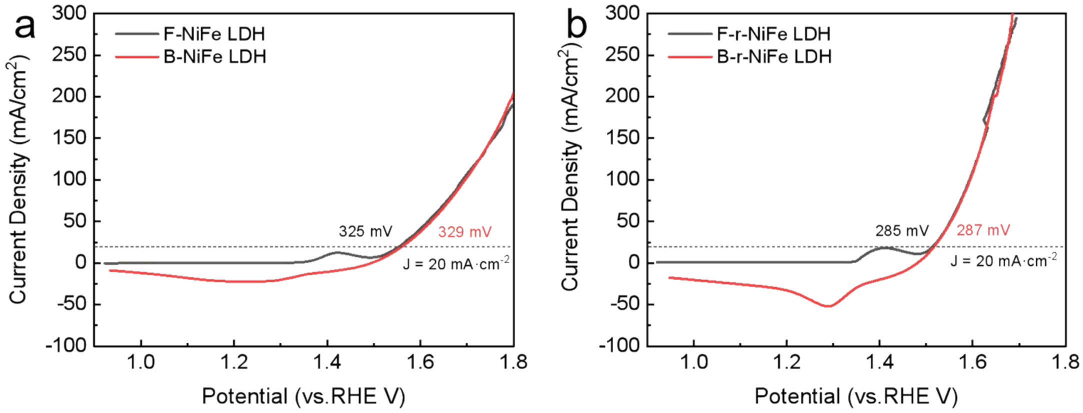

Fig. S15 Comparison between the LSV curves (from 0.9 V to 1.8 V) and CV measurement (from 1.8 V to 0.9 V) of (a) NiFe LDH, (b) r-NiFe LDH.

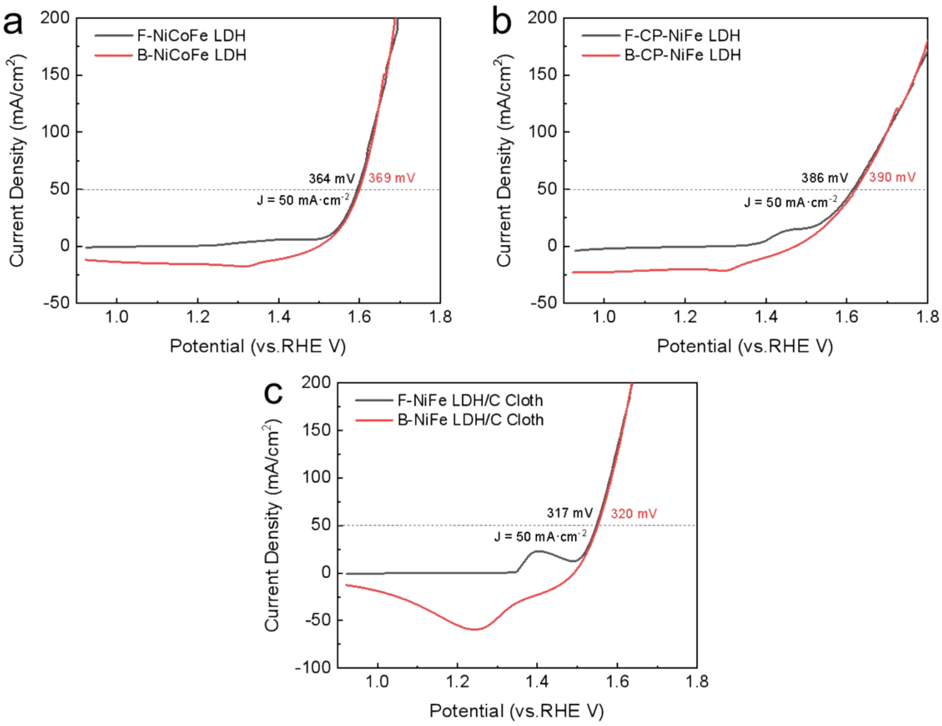

Fig. S16 Comparison between the LSV curves (from 0.9 V to 1.8 V) and CV measurement (from 1.8 V to 0.9 V) of (a) NiCoFe LDH, (b) CP-NiFe LDH, (c) NiFe LDH/C Cloth

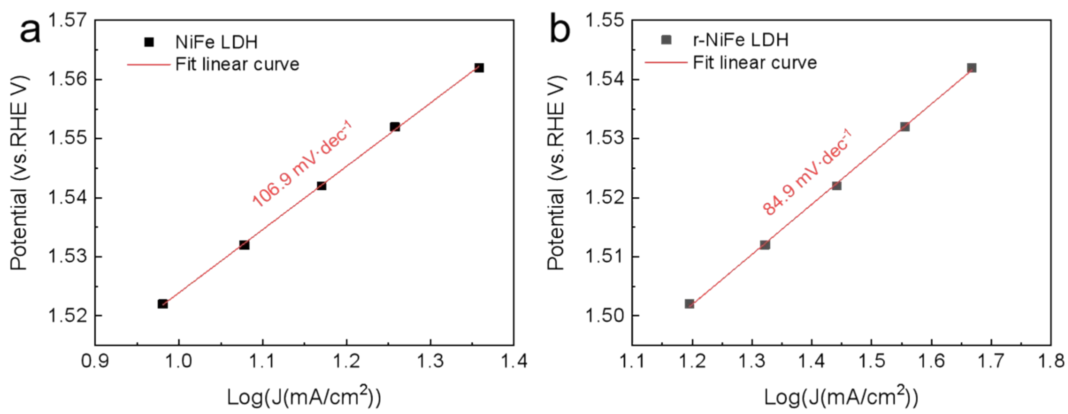

Fig. S17 Tafel slopes measured by steady-state polarization of (a) NiFe LDH, (b) r-NiFe LDH.

Table S3 ICP analysis of Ni and Fe in the KOH before and after 1000 cycles

Sample	Ni (μg/L)	Fe (μg/L)
Before 1000 cycles	17.2	39.0
After 1000 cycles	87.9	89.3

References

1. J. Li, T. Hu, C. Wang and C. Guo, *Green Energy Environ.*, 2020, DOI: 10.1016/j.gee.2020.11.009.
2. S. Klaus, M. W. Louie, L. Trotochaud and A. T. Bell, *J. Phys. Chem. C*, 2015, **119**, 18303-18316.
3. J. Zhang, H. Zhang and Y. Huang, *Appl. Catal. B*, 2021, **297**, 120453.
4. C. Chen, Z. Yang, W. Liang, H. Yan, Y. Tuo, Y. Li, Y. Zhou and J. Zhang, *J. Energy Chem*, 2021, **55**, 345-354.
5. Y. Wang, S. Tao, H. Lin, S. Han, W. Zhong, Y. Xie, J. Hu and S. Yang, *RSC Adv.*, 2020, **10**, 33475-33482.
6. X. Li, W. Q. Huang, L. X. Xia, Y. Y. Li, H. W. Zhang, S. F. Ma, Y. M. Wang, X. J. Wang and G. F. Huang, *ChemElectroChem*, 2020, **7**, 4047-4054.
7. Y. Lin, H. Wang, C. K. Peng, L. Bu, C. L. Chiang, K. Tian, Y. Zhao, J. Zhao, Y. G. Lin, J. M. Lee and L. Gao, *Small*, 2020, **16**, e2002426.
8. J. Liu, J. Zhou, S. Liu, G. Chen, W. Wu, Y. li, P. Jin and C. Xu, *Electrochim. Acta*, 2020, **356**.
9. W. Wang, Y. Liu, J. Li, J. Luo, L. Fu and S. Chen, *J. Mater. Chem. A*, 2018, **6**, 14299-14306.
10. Z. Lu, L. Qian, Y. Tian, Y. Li, X. Sun and X. Duan, *Chem Commun (Camb)*, 2016, **52**, 908-911.
11. X. Han, C. Yu, S. Zhou, C. Zhao, H. Huang, J. Yang, Z. Liu, J. Zhao and J. Qiu, *Adv. Energy Mater.*, 2017, **7**.
12. Y. Qin, F. Wang, J. Shang, M. Iqbal, A. Han, X. Sun, H. Xu and J. Liu, *J. Energy Chem*, 2020, **43**, 104-107.
13. Y. Dou, C.-T. He, L. Zhang, M. Al-Mamun, H. Guo, W. Zhang, Q. Xia, J. Xu, L. Jiang, Y. Wang, P. Liu, X.-M. Chen, H. Yin and H. Zhao, *Cell Reports Physical Science*, 2020, **1**.

14. H. Huang, C. Yu, X. Han, S. Li, S. Cui, C. Zhao, H. Huang and J. Qiu, *Ind. Eng. Chem. Res.*, 2017, **56**, 14245-14251.
15. H. Huang, C. Yu, C. Zhao, X. Han, J. Yang, Z. Liu, S. Li, M. Zhang and J. Qiu, *Nano Energy*, 2017, **34**, 472-480.
16. K. N. Dinh, X. Sun, Z. Dai, Y. Zheng, P. Zheng, J. Yang, J. Xu, Z. Wang and Q. Yan, *Nano Energy*, 2018, **54**, 82-90.
17. Y. Guo, C. Zhang, J. Zhang, K. Dastafkan, K. Wang, C. Zhao and Z. Shi, *ACS Sustainable Chem. Eng.*, 2021, **9**, 2047-2056.